Suspensions of Polymer-grafted Nanoparticles with Added Polymers - Structure and Effective Pair-interactions

Sivasurender Chandran[a,c], Shibu Saw[b,d], A. K. Kandar[a], C. Dasgupta[b], M. Sprung[e] and J. K Basu[a1, a)]

[a] *Department of Physics, Indian Institute of Science, Bangalore, 560012, India;*

[b] *Centre for Condensed Matter Theory, Indian Institute of Science, Bangalore, 560012, India;*

[c] *Institute of Physics, Albert–Ludwigs University of Freiburg, 79104, Freiburg, Germany;*

[d] *School of Chemistry, University of Sydney, Sydney, New South Wales, 2006, Australia;*

[e] *Deutsches Elektronen Synchrotron DESY, Notkestresse 85, 22607, Hamburg, Germany.*

(Dated: 28 July 2015)

We present the results of combined experimental and theoretical (molecular dynamics simulations and integral equation theory) studies of the structure and effective interactions of suspensions of polymer grafted nanoparticles (PGNPs) in the presence of linear polymers. Due to the absence of systematic experimental and theoretical studies of PGNPs, it is widely believed that the structure and effective interactions in such binary mixtures would be very similar to those of an analogous soft colloidal material - star polymers. In our study, polystyrene-grafted gold nanoparticles with functionality f =70 were mixed with linear polystyrene of two different molecular weights for obtaining two PGNP:PS size ratios, ξ= 0.14 and 2.76 (where, $\xi = M_g/M_m$, M_g and M_m being the molecular weights of grafting and matrix polymers respectively). The experimental structure factor of PGNPs could be modeled with an effective potential (Model-X), which has been found to be widely applicable for star polymers. Similarly, the structure factor of the blends with ξ=0.14 could be modeled reasonably well, while the structure of blends with ξ=2.76 could not be captured, especially for high density of added polymers. A model (Model-Y) for effective interactions between PGNPs in a melt of matrix polymers also failed to provide good agreement with the experimental data for samples with ξ=2.76 and high density of added polymers. We tentatively attribute this anomaly in modeling the structure factor of blends with ξ=2.76 to the questionable assumption of Model-X in describing the added polymers as star polymers with functionality 2, which gets manifested in both polymer-polymer and polymer-PGNP interactions especially at higher fractions of added polymers. The failure of Model-Y may be due to the neglect of possible many-body interactions among PGNPs mediated by matrix polymers when the fraction of added polymers is high. These observations point to the need for a new framework to understand not only the structural behavior of PGNPs, but possibly their dynamics and thermo-mechanical properties as well.

[a)]Electronic mail: basu@phyiscs.iisc.ernet.in

I. INTRODUCTION

In recent years, soft nanocolloids have generated significant interest, especially due to their tunable strength and range of interactions[1–5]. Their structural and dynamical phase behavior has been shown to be significantly more diverse and richer than that of corresponding hard sphere colloids[5–10]. Star polymers and polymer grafted nanoparticles (PGNPs) constitute an important class of such soft nanocolloidal particles, for which some work has emerged recently where the structure and dynamics of either the pristine colloids or their binary mixtures have been investigated[3,5–11,13–18]. Extensive research on star polymers over the last decade has led to the emergence of a reasonably good understanding of the microscopic origins of their observed phase behavior, including prediction and verification of an effective interaction potential between these entities[5,19–21]. Unfortunately, the same cannot be said for PGNPs, despite the fact that they are also widely accepted as a prototypical additive in polymer matrices to create novel functional polymer nanocomposites (PNCs)[1–4,15,22–27]. Understanding the phase behavior of such systems is of paramount importance given their enormous technological relevance. Several groups have reported structural, dynamical, thermal and mechanical properties of systems with different concentrations of PGNPs in a polymer matrix[1,3,4,6,7,15–17,23–28]. However, till date, with the exception of a recent investigation by Meng *et al.*[18] for PGNPs in polymer melt, no model effective interaction potential exists, probably because of the perception that this effective potential would be, essentially, same as that for star polymers due to their structural similarity[6]. Though there is a wealth of information on PGNP melts, surprisingly, very few studies of PGNPs in solution exist[10]. Such studies, especially the structural aspect, would be highly desirable to obtain insight into the nature of effective interactions between such soft nanocolloidal particles whose interaction could, presumably, be tuned by a range of parameters, such as graft chain length, density and core-to-corona size ratio or by using polymer additives of various sizes and concentrations.

It is now well accepted[1,2] that, if the graft and matrix chains are of similar chemical structure, then the structure of PGNP-polymer composites is controlled by entropic contributions which, in turn, are determined by a multitude of parameters, such as the grafting density, size ratio between particles and matrix polymers and that between matrix polymers and graft polymers. Initial simulation studies[18,29,30] confirm this picture. Recently,

we have shown that PGNPs in both melt[7] and concentrated solutions[10] exhibit unusual structure and dynamic behavior not seen in their conventional counterparts. The current work is motivated by these observations. We have studied the structure of suspensions of PGNPs with functionality f=70 and their mixtures with linear polymers having different size ratios, ξ =0.14 and 2.76 ($\xi = M_g/M_m$, where M_g and M_m are the molecular weights of the grafting and matrix polymers, respectively). These results have been obtained using small angle x-ray scattering (SAXS) measurements and molecular dynamics (MD) simulations. In the absence of any well-accepted effective potential for PGNPs, we have used two different effective potentials: (a) the potential developed by Likos and coworkers[21] for the interaction between star polymers and linear polymers (Model-X), and (b) the effective force between two PGNPs dispersed in a dense polymer matrix, obtained by Kumar and coworkers[18] (Model-Y). Both these potentials are found to provide a reasonable description of the behavior of mixtures for ξ =0.14, but the behavior of systems with ξ =2.76 could not be captured for blends with high concentrations of added polymers. Based on our MD simulation results and effective interactions between PGNPs in polymer mixtures obtained from Model-X using integral equation theory (IET), we suggest that the failure of the models for higher densities of added polymers is due to questionable assumptions in both models, viz., simplified description of a linear polymer as a star polymer with f=2 in Model-X and the limitation of considering only two PGNPs in the simulations used to construct Model-Y. This observation indicates the need for better models for understanding the effective interactions and phase behavior of PGNP systems.

II. METHODS

A. Sample preparation and sample details

The results presented here are based on concentrated solutions (concentrations of the order of the overlap concentration, C^* and above) of binary mixtures of PGNPs and linear polymers in toluene. Gold nanoparticles grafted with thiol terminated polystyrene were synthesized using methods described earlier[6,7,31]. The PGNPs were well characterized by various techniques such as transmission electron microscopy (TEM), thermogravimetric analysis (TGA) and dynamic light scattering (DLS). TEM images of the PGNPs along with the

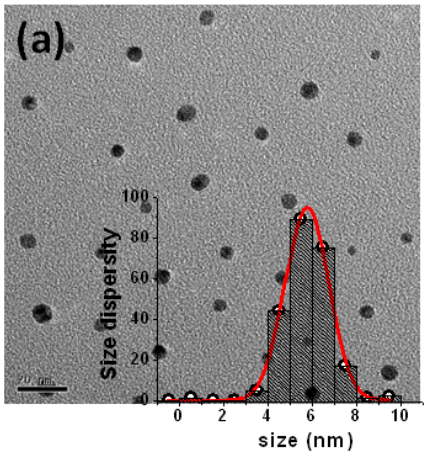

FIG. 1. Transmission electron micrograph of a PGNP sample. Inset: A histogram for the size distribution and a Gaussian fit (continuous line) are shown, from which the mean size and the polydispersity of the PGNPs were derived.

corresponding histogram for indicating the size polydispersity are shown in the Fig-1. The hydrodynamic radius, R_h, of PGNPs was obtained from DLS.

The functionality f of the PGNPs are obtained using the following relation,

$$f = \frac{N_{chain}}{N_{core}} \tag{1}$$

where, N_{chain} is the total number of chains for a given mass of the PGNPs, and N_{core} is the total number of cores. N_{chain} and N_{core} can be found using the equations (2) and (3), based on the experimental parameters

$$N_{chain} = \frac{W_g N_A}{M_g} \tag{2}$$

$$N_{core} = \frac{W_{Au}}{4/3\pi R_c^3 \rho_{Au}} \tag{3}$$

where W_{Au} and W_g are the masses of gold core and grafting polymer as obtained from TGA, M_g is the molecular weight of the grafting polymer and R_c is the radius of the gold core (obtained from TEM). The defining characteristics of both the PGNPs are tabulated in Table-I.

In the melt state, two important factors define the dispersion state of a particle in a polymer matrix[1,2,23]: Entropy of mixing and stretching energy of matrix polymer chains. The entropy of mixing or the configurational entropy always favors dispersion. On the other hand, to accommodate a particle the matrix chains have to stretch, costing an energy penalty which increases with increasing particle radius. For particles grafted with polymer chains, the graft/matrix interactions are primarily dependent on the grafting density, M_g and M_m. In our case, the grafting density is constant and hence the relative molecular weights should play a deciding role in the graft/matrix interactions. When, $M_g > M_m$ (ξ >1), the matrix chains can interpenetrate with the graft chains and wet the graft layer. On the other hand, for $M_g < M_m$ (ξ <1), the host chains have to pay a higher cost to interpenetrate with the graft chains. This induces an excluded volume around the PGNP-polymer interface which in turn creates a driving force for the PGNPs to aggregate (for minimizing the contact area). This eventually creates a macro/micro phase separated state.

To understand the importance of ξ on the structure of PGNPs-polymer suspensions, we have chosen two different molecular weights for the linear polystyrene for obtaining two different ξ values, ($\xi < 1$ and $\xi > 1$). PGNPs were dissolved in toluene by constant stirring to form homogeneous solutions. The linear polymers (polystyrene of molecular weights 19.2 and 382 kg/mol) were also dissolved in toluene in similar way. For all the mixtures, the fraction of PGNPs was fixed at 0.17. The solutions (PGNP in toluene and PS in toluene) were then mixed in various proportions to obtain the samples described in Table-II. To make it easier to remember the absolute concentration of polymer in the PGNP-polymer suspensions, we have named the samples in the following way: Yi, where, Y denotes the molecular weight of the polymer added in relation to the molecular weight of the grafting agent i.e., H for higher molecular weight (382 kg/mol) and L for lower molecular weight (19.2 kg/mol). The number index i denotes the relative concentration of the polymers added. For examples H1 contains less polymer than H2, which in turn contains less polymer than H3.

B. Small angle X-ray scattering measurements

Small angle x-ray scattering measurements were performed at the P-10 beamline of PETRA-III, Deutsches Elektronen Synchrotron (DESY) at a temperature of 190 K using X-ray beam of energy 8.0 keV. For collecting the SAXS data, the suspensions were

TABLE I. Properties of PGNPs

R_c	M_g	R_h	f
nm	*kg/mol*	*nm*	
2.9	53	32.2	70

R_c is the radius of the core (gold nanoparticles), M_g is the molecular weight of the grafting polymer, R_h is the hydrodynamic radius of the PGNP and f is the functionality of a PGNP.

filled in capillary tubes (of diameter 1 mm). A beam size of $20\times20\mu m^2$ was used for the measurements and the scattered beam was recorded on Pilatus 300K detector as described elsewhere[32]. As PGNPs are athermal systems, the temperature is not expected to play any significant role in determining the nature of the interactions. In general, the scattered intensity can be written as,

$$I(q, N_p) = N_p \Delta\rho^2 P(q) S(q, N_p) \tag{4}$$

where q is the scattering wave vector, N_p is the number of PGNPs (considering only the gold cores), $\Delta\rho(=\rho_{Au} - \rho_{PS})$ is the scattering contrast, $P(q)$ is the form factor of PGNPs and $S(q, N_p)$ is the structure factor. The form factor $P(q)$ depends on the shape and size of the basic scattering entities, which in our case are the PGNPs. As described earlier, the shape and size of the PGNPs have been determined using TEM (Fig-1). TEM images of the PGNPs clearly remove the shape effect as the PGNPs are quite spherical. At infinite dilution ($N_p \to 1$), the scattering due to the inter particle correlations can be neglected and only the size and shape of the PGNPs contribute to the scattering. Hence,

$$I(q, N_p)_{N_p\to1} \approx \Delta\rho^2 P(q) \tag{5}$$

A common functional form for fitting $P(q)$ of the star polymers is given by Alessandrini and Carignano[33] and Beaucage[34,35]:

$$P(q) = \exp\left[-\frac{(qR)^2}{3}\right] + \frac{B}{V_w}\left[\frac{\mathrm{erf}(1.06qR/\sqrt{6})^3}{qR}\right]^d \tag{6}$$

TABLE II. Specification of binary mixtures of PGNPs and PS

Sample	M_m kg/mol	C/C^*	ξ	λ
L1	19.2	0.8	2.76	0.15
L2		3.0		
L3		12.0		
H1	382	1.5	0.14	0.85
H2		3.0		
H3		6.0		

Size asymmetry, λ=$R_h^{polymer}/R_h$, $R_h^{19.2k}$ is 4.7 nm and R_h^{382k} is 27.5 nm. $C^*_{19.2k}$ =180 mg/ml and C^*_{380k} = 18.57 mg/ml.

where, V_w, R denote the molar volume and radius of gyration of the scattering entity, respectively. The exponent d defines the fractal dimension of the scattering entities; $4 > d > 3$ for surface fractals, $d < 3$ for mass fractals and $d > 4$ for diffuse interfaces. The first term in the right hand side is the Guinier term denoting the longest length scale (lower q) responsible for scattering, whereas the second term that dominates at higher q or at small length scale represents monomer correlations. The prefactor B of the second term depends on the excluded volume interactions and its screening. We will use equation (6) for modeling the form factor of PGNPs, treating V_w, R, B and d as fit parameters. .

Using equations (5) and (4), we obtain the following expression for the structure factor $S(q, N_p)$:

$$S(q, N_p) \approx \frac{1}{N_p} \frac{I(q, N_p)}{I(q, N_p)_{N_p \to 1}} \tag{7}$$

For convenience, $S(q, N_p)$ will be written as $S(q)$ throughout the paper. The primary peak position, q^*, of the structure factor $S(q)$ provides a measure of the inter-particle spacing between PGNPs.

C. Simulation Details

We have performed constant total number of particles (PGNPs or PGNPs and matrix polymers), volume and temperature (NVT) MD simulations for 1000 to 8800 particles. The temperature was kept fixed using the Brown-Clarke thermostat[36]. Periodic boundary conditions were used in all three directions. As briefly mentioned earlier, we have performed MD simulations using two model potentials for the binary mixtures. a) Model-X, which is a model potential for star polymers in polymer matrix, with explicit forms for the interactions between star polymer-star polymer, linear polymer-linear polymer and star polymer-linear polymer. This model has been adapted from Ref.[21]. PGNPs are assumed to behave as star polymers in our computations[6]. b) Model-Y, which is a model potential[18] that describes the effective force between two PGNPs dispersed in a dense matrix of polymers. This model has been adapted from Ref.[18]. For the sake of completeness we describe both the models and the evaluation of different parameters, especially for Model-Y.

In the first model potential[21] (Model-X), the PGNP-PGNP effective interaction, in a good solvent, is given by[21]

$$\frac{V_{nn}(r)}{k_BT} = \Psi(f) \begin{cases} -\ln(\frac{r}{\sigma_n}) + \frac{1}{1+\frac{\sqrt{f}}{2}} & r \leq \sigma_n \\ \frac{\sigma_n}{r(1+\frac{\sqrt{f}}{2})} \exp\Big[-\frac{\sqrt{f}}{2\sigma_n}(r-\sigma_n)\Big] & r > \sigma_n \end{cases} \tag{8}$$

where $\Psi(f) = (5/18)f^{3/2}$, σ_n is the corona diameter of a PGNP, f is the functionality and k_B is the Boltzmann constant.

In Model-X, a linear polymer has been modeled as a star polymer with $f = 2$[21]. The potential form of star polymers with small f differs from that with large f only at large distances where it decays as a Gaussian rather than a Yukawa form. The corresponding polymer-polymer interaction form is given as[37]

$$\frac{V_{pp}(r)}{k_BT} = \Psi(2) \begin{cases} -\ln(\frac{r}{\sigma_p}) + \dfrac{1}{2\mu^2\sigma_p^2} & r \leq \sigma_p \\ \dfrac{1}{2\mu^2\sigma_p^2} \exp\Big[-\mu^2(r^2-\sigma_p^2)\Big] & r > \sigma_p \end{cases} \tag{9}$$

where $\mu = 1.03/\sigma_p$ and σ_p is a measure of the size of a polymer.

The PGNP-polymer interaction is given as[38]

$$\frac{V_{np}(r)}{k_BT} = \begin{cases} \hat{\Psi}(f)\ln(\frac{r}{\sigma_{np}}) + K & r \le \sigma_{np} \\ \nu_0 \int \phi_n(r')\phi_p(|\mathbf{r}-\mathbf{r}'|)d\mathbf{r}' & r > \sigma_{np} \end{cases} \tag{10}$$

where $\hat{\Psi}(f) = \frac{5}{36}\frac{1}{\sqrt{2}-1}[(f+2)^{3/2} - (f^{3/2}+2^{3/2})]$, $\sigma_{np} = (\sigma_n + \sigma_p)/2$, and

$$\frac{\phi_\alpha(r)}{A_\alpha} = \begin{cases} (\frac{\sigma_\alpha}{2})^{-5/3} r^{-4/3} & r \le \frac{\sigma_\alpha}{2} \\ (\frac{1}{r^2} + 2\kappa_\alpha^2)\frac{2\zeta_\alpha}{\sigma_\alpha}\exp\left\{\kappa_\alpha^2[(\frac{\sigma_\alpha}{2})^2 - r^2]\right\} & r > \frac{\sigma_\alpha}{2} \end{cases} \tag{11}$$

Here, $\zeta_\alpha = \frac{1}{1+\kappa_\alpha^2\sigma_\alpha^2/2}$ and A_α is a normalization constant. We have used $\kappa_\alpha = 1.27/\sigma_\alpha$ following Ref.[21]. K and ν_0 are constants whose values are determined by the requirement of the continuity of $V_{np}(r)$ and its first derivative at $r = \sigma_{np}$.

All quantities are expressed in reduced unit. Unless stated otherwise, time and length are expressed in unit of $\sqrt{m_n\sigma_n^2/k_BT}$ and σ_n, respectively, where T is the temperature. Time steps $dt = 0.005$ were used in our MD simulations. The systems were first equilibrated for 1-4 million MD steps and various quantities of interest were calculated from production runs of 1-4 million time steps. For Model-X, we have used $N = 2000$ for pure PGNPs in our simulations. We compared the results for $N = 2000$ and $N = 1000$ and no system size effect was observed. This is intuitive since the density of pure PGNPs (0.17 in reduced units) is small. For PGNP-polymer suspensions, we have performed MD simulations using $N = 5500$ to $N = 8800$ particles (PGNP+polymer). The exact numbers of PGNPs and matrix polymers used in our simulations have been shown in Table III. We have compared the structure factors obtained for both Model X and Model Y using the Brown-Clarke thermostat with those obtained in the microcanonical ensemble and found no difference between the two sets of results. This clearly indicates that the structures obtained from our simulations are not sensitive to fluctuations in the kinetic energy which are neglected in the isokinetic Brown-Clarke thermostat.

In the second model potential (Model-Y), we adapt the effective force between two PGNPs obtained by Meng et.al.[18]. They obtained the effective force from bead-spring coarse-grained MD simulations in the presence of a large density of matrix polymers. The effective form of the force is found to depend on the size ratio ξ. For $\xi = 1$, the form of the effective force is a power-law, which is given as

TABLE III. Parameters for simulations using model-X. N_n and N_p are the number of PGNPs and polymers respectively.

Sample	$N = N_p + N_n$	N_p
Pure PGNP	2000	0
H1	8800	1467
H2	8800	2200
H3	8800	4400
L1	5500	5000
L2 sample1	6400	6000
L2 sample2	6300	6000
L2 sample3	5100	5000
L2 sample4	7100	7000

TABLE IV. Parameters for the repulsive form of model-Y, $F(r) = (a/r)^b$. N is the number of particles in the simulated sample.

Sample	a	b	N
L1	1.40	12	1000
L2	1.50	12	1000

$$F(r) = \left(\frac{a}{r}\right)^b. \tag{12}$$

In this expression, the distance r is measured in units of σ, the "monomer size", and a is the size of a PGNP in the same unit. A prefactor of dimension [energy]/[length] has been set to unity, thereby defining the scale of the temperature. In our simulations, we have used a cut-off of $a/[4.5^{-12}(b-1)/a]^{1/(b-1)}$. This cut-off ensures that the value of the potential at the cut-off is the same as that in the case of a potential of the form $(a/r)^{12}$ with cut-off $4.5a$. Table-IV shows the different parameters values and particle numbers used to simulate PGNPs. These parameter values have been obtained by trial and error.

For $\xi = 1/7$, the effective force takes the form[18]

TABLE V. Parameters for the attractive version of model-Y, $F(r) = \left[\left(\frac{a}{r}\right)^b - \left(\frac{a}{r}\right)^c\right] \exp(d - er)$. N is the number of particles in the simulated sample.

Sample	a	b	c	d	e	N
H1, H2, H3	10.59	4	1.23	4.65	0.36	1000

s

$$F(r) = \left[\left(\frac{a}{r}\right)^b - \left(\frac{a}{r}\right)^c\right] \exp(d - er) \tag{13}$$

where the lengths r, a, and e^{-1} are measured in units of σ and the values of a, b, c, d and e are obtained from fits of the effective force data to this form. In this case, a cut-off of 30 (in units of σ) has been used. Table-V shows the different parameter values obtained from fitting the effective force data of Ref[18] with the above function for $M_g = 10m_0$ and $M_m = 70m_0$ *i.e.* $\xi = 1/7$, where m_0 is the monomer mass of polystyrene or grafted polymer. We have used a grafting density $\Sigma = 0.76$ chains/σ^2 which corresponds to $f = 60$ in Model-Y while in our experimental system, the values of f is 70. Simulations with Model-X has been performed with $f = 73$. A small difference in f should not have any significant effect on the structure of PGNP composites.

D. Integral Equation Theory

The radial distribution function $g_{\alpha\beta}(r)$ of PGNP-polymer mixtures was obtained by solving the Ornstein-Zernike[39,40] equation

$$h_{\alpha\beta}(r) = c_{\alpha\beta}(r) + \sum_{\nu\in(\alpha,\beta)} \rho_\nu \int c_{\alpha\nu}(|\mathbf{r} - \mathbf{r}'|) h_{\nu\beta}(r') d\mathbf{r}' \tag{14}$$

where $h_{\alpha\beta}(r) = 1 - g_{\alpha\beta}(r)$ and $c_{\alpha\beta}(r)$ is the direct correlation function, along with Rogers-Young(RY)[41] closure, which is an interpolation between Percus-Yevick[42] and hypernetted-chain (HNC) closures and is given by

$$g_{\alpha\beta}(r) = e^{-\phi_{\alpha\beta}(r)/(k_B T)} \left[1 + \frac{e^{f(r)[h_{\alpha\beta}(r) - c_{\alpha\beta}(r)]} - 1}{f(r)}\right], \tag{15}$$

where f(r) is a "switching parameter" that can be written as

$$f(r) = 1 - e^{-\alpha_{RY} r}. \tag{16}$$

The value of α_{RY} is determined from thermodynamic consistency, i.e. by requiring that the compressibility obtained using the virial equation of state is the same as that from the compressibility equation of state[40,43]. Equations (14) and (15) are solved iteratively to obtain $g_{\alpha\beta}(r)$.

Once the radial distribution function $g_{\alpha\beta}(r)$ is determined, the structure factor can be estimated as[40]

$$S_{\alpha\beta}(q) = x_\alpha \delta_{\alpha\beta} + x_\alpha x_\beta \rho \int (g_{\alpha\beta}(r) - 1) e^{-\mathbf{iq.r}} d\mathbf{r} \tag{17}$$

where $x_\alpha = \frac{N_\alpha}{N}$ is the concentration of α species, N_α being the number of α particles.

III. RESULTS AND DISCUSSIONS

A. Experiments

Small angle x-ray scattering data for PGNP suspensions were collected for various concentrations of PGNPs (ϕ_p) in toluene. The data for five representative concentrations are shown in Fig-2(a). The peaks observed in Fig-2(a) denote the inter-particle spacings of PGNPs at the respective concentrations. It could be observed that with increasing concentration the peak shifts to a higher q indicating a reduction in inter-particle spacing, as expected for homogeneous systems. As described earlier, the scattering data for dilute suspensions, where multiple scattering effects could be safely neglected, provide information about the molecular weight, size, shape and mass distribution. The scattering data for a dilute PGNP suspension is fitted to equation (6), as shown in Fig-2b. R obtained from fitting the data is 170 nm, which is close to the expected mean inter-particle distance at the fraction used. From Fig-2(b), it is clear that the form factor of the PGNPs could be well described by eq. (6), which is originally developed for star polymers. This observation establishes the structural similarity of PGNPs with star polymers. The scattering data ($I(q)$ vs q) for the fraction $\phi_p = 0.02$ is used as $P(q)$ for obtaining the $S(q)$ for other samples (see eq. (7)).

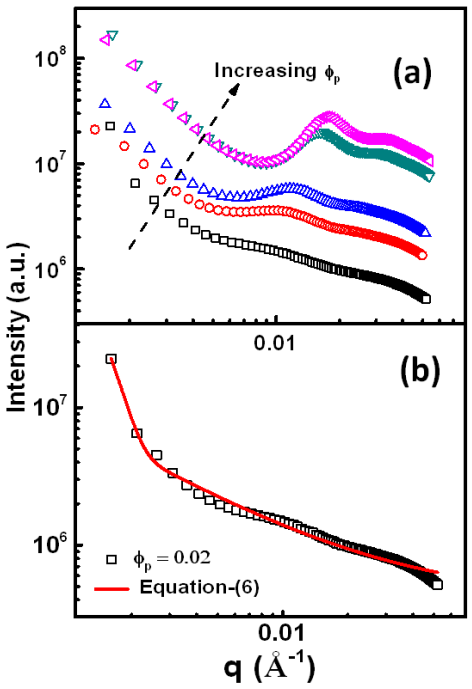

FIG. 2. (a) SAXS data (Intensity vs. the wave vector q) of the PGNPs for five different concentrations viz., ϕ_p=0.02 (square), 0.035 (circle), 0.05 (upward facing triangle), 0.12 (left facing triangle) and 0.15 (downward facing triangle). (b) Experimental data (open squares) for a PGNP-solution with a concentration ϕ_p=0.02 are shown along with the best fit (continuous line) to the form in equation (6).

For the investigation of binary mixtures, the volume fractions of pure PGNP solutions is kept constant at 0.17 which corresponds to an interparticle spacing of 26±3 nm, which is approximately half of the hydrodynamic diameter $2R_h$ (see table-1 for the R_h value) of the PGNPs. These concentrations ensure a sufficiently strong overlap between the PGNPs allowing for manifestations of the effective interaction, and its possible modifications due to added polymers, through their structure. Figure-3 shows the $S(q)$ for all the PGNP-polymer suspensions (see Table-II for the concentrations of polymers) studied in this work. The structure factor $S(q)$ provides information about the structure of PGNPs and polymers in the suspension. The position of the first $S(q)$ peak (q^*) can be used to obtain the inter-particle spacing, d, i.e. $d = 2\pi/q^*$. The inter-particle spacing obtained for the pure PGNP suspensions is 30±1 nm. The inter-particle spacing calculated from the initial volume fraction is, within the error, the same as the spacing obtained from the value of q^*. This indicates that the PGNPs in the pristine PGNP suspension (without added polymers) are homogeneously

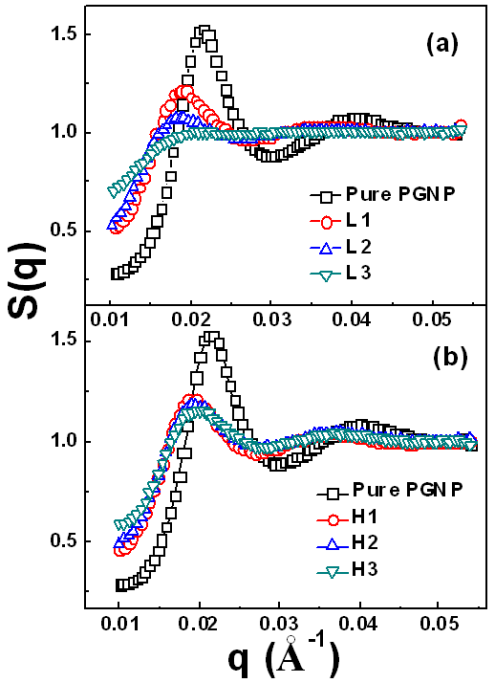

FIG. 3. Structure factor $S(q)$ vs the wave vector q for PGNP-polymer suspensions with polymers of molecular weight 19.2 kg/mol [panel (a)] and 382 kg/mol [panel (b)]. See Table-II for the sample details.

dispersed and the possibility of formation of any clusters can be safely omitted.

Now let us turn our attention to the structure of PGNP-polymer suspensions. The $S(q)$ data for all the PGNP-polymer suspensions were obtained by normalizing the scattering data with the $P(q)$ of PGNPs and are shown in Fig-3(a,b). For the mixtures with both higher (H) and lower (L) molecular weight of the added polymers, with the addition of minimum density of polymers (L1, H1) the position of the first peak of $S(q)$ shifts towards lower q and the height of the first peak decreases. The shift in q^* indicates a homogeneous distribution of PGNPs and polymers, while the diminishing peak height of $S(q)$ indicates that the addition of polymers perturbs the core-core correlations i.e. the system gets disordered. Upon further addition of polymers there are no obvious shifts in the peak to lower or higher q i.e. there is no significant difference in the q^* between the samples from $L1 - L3$ and $H1 - H3$. For a homogeneous dispersion of PGNPs and polymers, the q^* is expected to further shift towards lower q. The fact that this is not observed might indicate the formation of clusters or domains of PGNPs in the suspension. For other similar systems like colloid-polymer mixtures and star polymer-polymer mixtures, it is well known that with increasing fraction of added

polymers, depletion induced attraction between the colloids (or star polymers) leads to phase segregation and eventual shift in the $S(q)$ peak to higher q values[15,44–47]. For systems with depletion interactions, it is shown that the height of the primary peak of $S(q)$ increases with increasing the fraction of added polymers while q^* simultaneously shift to higher q values. Such features are absent in our structure factors. Hence, the presence/absence of depletion induced attractions is not sufficiently clear from the data. This aspect will be discussed later after considering the simulation results. It is also important to note that with the addition of polymers, $S(q)$ behaves similarly for both $\xi < 1$ (H) and $\xi > 1$ (L). For PNCs, the $\xi < 1$ regime leads to aggregation of PGNPs while the opposite regime leads to the formation of stable dispersions. Hence one would have expected to see corresponding signatures in $S(q)$, but the data do not show any qualitative difference between the behavior of $S(q)$ for $\xi < 1$ and $\xi > 1$. It is possible that our $S(q)$ data obtained for relatively large values q do not pick up the signatures of the occurrence of aggregation of PGNPs in the $\xi < 1$ cases. The simulation results described in the next section provide important information about this possibility.

B. Simulations

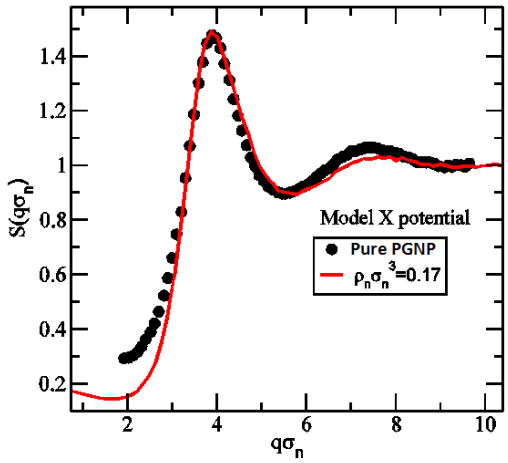

FIG. 4. Comparison of the structure factor of pure PGNP solution, obtained from experiment and simulation using Model-X. The closed circles are the experimental data and the continuous line is the $S(q)$ generated by simulation. ρ_n and σ_n denotes the number density and diameter of the PGNPs. The polydispersity used in the simulation is 20%.

As described earlier, there is a scarcity of model potentials that can be used in simulations for determining the collective properties of PGNPs. In this work we use two existing model potentials: Model-X and Model-Y as defined in section II C. Before describing the simulation results, it is important to discuss the applicability of these two model potentials. In PGNPs the polymers are grafted to a small inorganic core and for large thickness of shells, the effect of the inorganic core will be minimal. Hence the structure should be dominated by the shells and PGNPs are expected to behave like star polymers. The form factor modeling (Fig-2b) for the PGNPs confirms the structural similarity of PGNPs with star polymers. In this context, by varying the functionality f, we have shown[7] that the diameter of the PGNPs scale with f in a fashion expected for star polymers[5]. Hence Model-X, which was originally developed for star polymers could potentially be used for PGNP suspensions. Model-Y is developed exactly for PGNPs, but the limitation is that the effective force is obtained by simulating not many but only two PGNPs dispersed in a matrix of polymers. Knowing these limitations, we have performed MD simulations using both the models and compared the obtained structural properties with those determined from experiments. For the attractive form of Model-Y (Eq. (13)), we have used the parameters obtained by fitting the force form shown by Meng *et al* for $\xi = 1/7$[18]. For the repulsive power-law form of Model-Y (Eq. (12)) we have performed the simulations for several set of values of model parameters that are close to the values expected for the experimentally studied systems. The results reported below correspond to parameter values for which closest agreement with experimental results was obtained.

In simulations, the structure factor $S(q)$ has been obtained from density correlation function in Fourier space[40]

$$S(q) = \frac{1}{N} < \rho_{\mathbf{q}} \rho_{-\mathbf{q}} > \tag{18}$$

where $\rho_{\mathbf{q}}$ is the number density in Fourier space and $< \cdots >$ indicates time averaging. This expression can be rewritten as

$$S(q) = \frac{1}{N} < \sum_{i,j} \exp[-\mathrm{i}\mathbf{q}.\mathbf{r}_{ij}] > \tag{19}$$

where $\mathrm{i} = \sqrt{-1}$ and $\mathbf{r}_{ij}$ is the displacement between the positions of i^{th} and j^{th} particles.

Figure- 4 exhibits a comparison of the experimental structure factor $S(q)$ of pure PGNP solution with the results of MD simulations based on Model-X. The MD simulations have

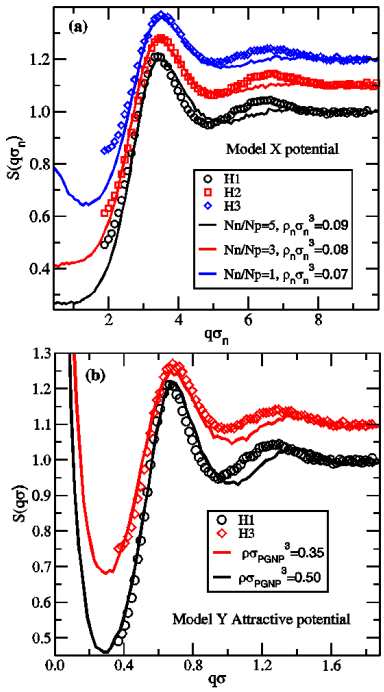

FIG. 5. Structure factor S(q) of H samples in comparison with the data obtained through simulations using (a) Model-X and (b) the effective attractive force of Model-Y. The data are shifted vertically by 0.10 for clarity. In (a) ρ_n represent the number density of PGNPs and N_n and N_p are the numbers of PGNPs and matrix polymers, respectively. The size ratio σ_n/σ_p is taken to be 1. The polydispersity used in these simulations is 20%. In (b), ρ is the number density of PGNPs and $\sigma_{\rm PGNP}$ is the size of a PGNP, taken to be equal to the parameter a in Model-Y. The wavenumber q in (b) is measured in units of $1/\sigma$, where σ is the monomer size.

been performed using the interactions given in Eq. (8). The $S(q)$ obtained from MD simulation at dimensionless density $\rho_n\sigma_n^3 = 0.17$ compares reasonably well with that obtained in the experiment except for low q. In these simulations, the PGNPs have been assumed to have a size polydispersity of 20%, which is close to the experimental polydispersity in the core diameter (see Fig-1). Polydispersity of the molecular weights of graft and matrix polymers is also known to produce significant effects in the potential of mean force between PGNPs[48]. However, due to the narrow width of the distribution of the molecular weights of the polymers (the polydispersity index of both graft and matrix polymers is ~ 1.06), we do not expect polydispersities of graft and matrix polymers to play any significant role in the experimentally studied samples. For this reason, polydispersity of the sizes of graft and matrix polymers was not considered in our simulations. The size of PGNPs, in simulations with

Model-X, have been taken from a Gaussian distribution with mean 1.0 and variance 0.20. The $S(q)$ has been determined for all particles as is the case in experimental evaluation of the structure factor. The value of σ_n used to bring the experimental results for $S(q)$ (in particular, the first peak position of $S(q)$) in agreement with the MD results is $\sigma_n = 18.55\ nm$. This value of σ_n obtained from the simulation is smaller than the experimentally determined hydrodynamic diameter of the PGNPs.

Fig. 5(a) shows a comparison of $S(q)$s obtained from experiments and simulations (using Model-X) for samples H1, H2 and H3. Both the height and the position of the first $S(q)$ peak obtained from simulations are in good agreement with the experimental results. However, the simulation is not able to capture properly the evolution of the second peak of $S(q)$. The value of σ_n used to bring the experimental results for q^* in agreement with those from simulations is $\sigma_n = 17.93\ nm$, which is close to the value for the case of pure PGNPs. The $S(q)$s obtained from simulations exhibit an upturn for small q, which is an indication of the formation of clusters. The values of $S(q)$ at the lowest q values are small compared to the values expected for bulk phase separation. Fig. 5(b) depicts the comparison of $S(q)$ obtained from experiment with that from MD simulations using the attractive effective force of Model-Y. The results for samples H1 and H3 have been compared with the experimental results. For these cases, we have performed simulations with the force form shown Eq. (13) with parameter values as shown in Table V. No polydispersity has been used in simulations with Model-Y. The two $S(q)$s are in good agreement with each other except that the simulation is not able to capture the second peak of the experimentally determined structure factor. We have used $\sigma = 3.5\ nm$ to bring the first peaks of the experimental and numerical $S(q)$s together, which implies that the size of a PGNP is $a\sigma = 37.07\ nm$, in reasonable agreement with the experimentally determined value. The systems in MD simulations are homogeneous irrespective of whether we use Model-X or Model-Y. The values of $S(q)$ even at the smallest q are of order of unity, thus removing the possibility of large-scale instabilities or phase separation. The formation of small clusters is visible in snapshots (not shown here) of the system. Also, experimentally on increasing the density of added polymers for H systems, the position of the first peak of $S(q)$ does not change. This is possible only if there is formation of clusters or if the system tends to phase-separate, while simulations clearly eliminate the second possibility.

In real space, the structure of a system can be studied through the radial distribution

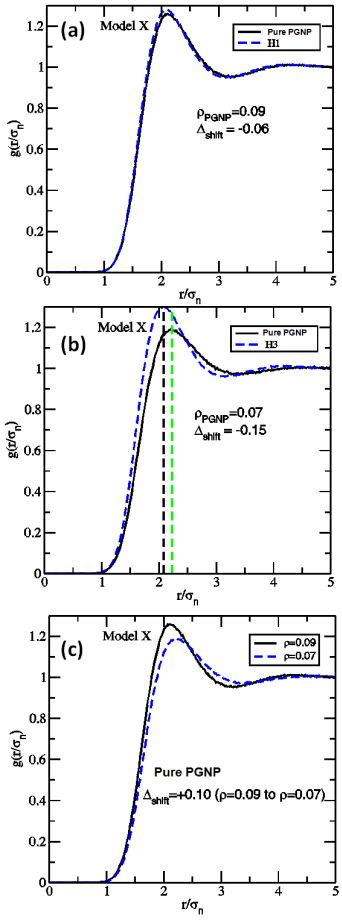

FIG. 6. The peak position of the radial distribution function, $g(r)$, in simulations performed using Model-X, shifts towards left due to depletion forces when pure PGNPs are immersed in a polymer matrix of different density [panels (a) and (b)]. This shifts is more prominent for the H3 case, where the density of matrix polymer is higher compared to H1. The rightward shift in the peak position of $g(r)$ due to lowering of density is illustrated in panel (c). The leftward shift due to depletion from H1 to H3 (-0.15+0.06=-0.09) is counterbalanced by the rightward shift due to density lowering (+0.10).

function $g(r)$, which is related to the Fourier transform of the structure factor, $S(q)$. Fig. 6(a) shows that the position of the first peak of $g(r)$ shifts to the left by $\Delta_{shift} = -0.06$ (-ve sign for leftward shifting) for H1 case in Model-X simulations. This shift is caused by the presence of depletion forces. The leftward shift is more prominent in going from pure PGNP to H3 case (Fig. 6(b)) due to larger polymer matrix density. The value of the shift for H3 case is $\Delta_{shift} = -0.15$. So, the net leftward shift from H1 to H3 is $\Delta_{shift} = -0.09$. However, the density of PGNP decreases from H1 to H3 cases from $\rho = 0.09\sigma_n^-3$ to $\rho = 0.07\sigma_n^-3$.

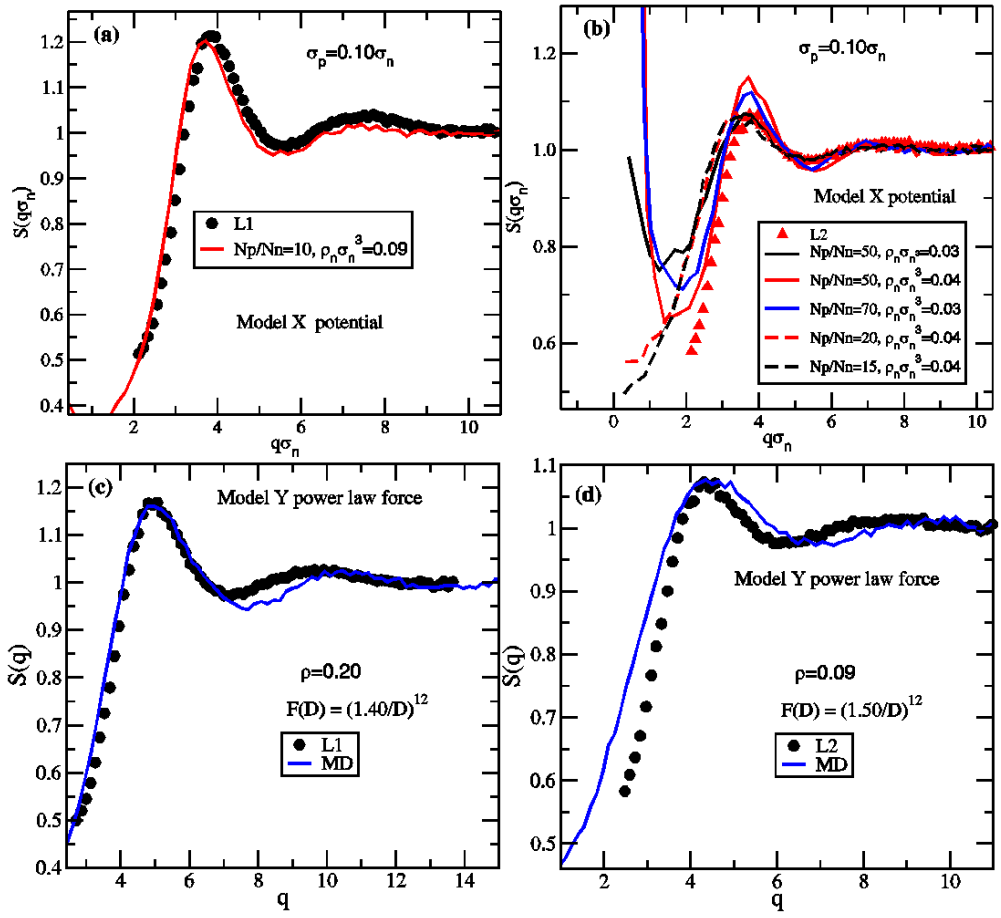

FIG. 7. The structure of pure PGNPs in small sized matrix polymer (a) L1 (Model-X), (b) L2 (Model-X), (c) L1 using the power-law force of Model-Y and (d) L2 using the power-law force of Model- Y.

Fig. 6(c) shows the shift of the peak position of $g(r)$ for pure PGNP A when the density is lowered from $\rho = 0.09\sigma_n^-3$ in H1 case to $\rho = 0.07\sigma_n^-3$ in H3 case. The shift is rightward contrary to the shifts in Fig 6(a) and (b).This shift $\Delta_{shift} = +0.10$ counterbalances the leftward shift caused by depletion forces in going from H1 to H3. Therefore, the positions of the peaks of $g(r)$ and $S(q)$ are essentially the same for H1 and H3 cases. This suggests that depletion interactions, as predicted for star polymer-linear polymer mixtures, also exist in the PGNP-linear polymer mixtures.

Now let us now turn to L series systems *i.e.* PGNPs in the presence of matrix polymers of size smaller than that of the grafted polymers ($\xi > 1$). Fig. 7(a) shows the comparison between the structure factors obtained from experiments and MD simulations, using Model-X potential for L1. In the simulations, the polymer to PGNP size ratio is taken to be 0.10

and the PGNP density is $\rho_n\sigma_n^3 = 0.09$. The $S(q)$ generated through MD simulations is in good agreement with the experimental data. Figure 7(b) depicts the comparison between structure factors obtained from experiment and MD simulations using the Model X potential for L2. The ratio of the numbers of matrix polymers and PGNPs varies from 15 to 70 and PGNP densities of $\rho_n\sigma_n^3 = 0.03$ and 0.04 have been considered in the simulations. For this case, none of the $S(q)$ obtained from MD simulation matches well with that from the experiment. Now let us consider the results of simulations using the effective force of Model-Y. The size ratio of grafted and matrix polymers is larger than unity in the experiment. It is shown in Ref.[18] that for size ratio $\xi < 1$, the effective force is of Lennard-Jones-type with an attractive well and for $\xi = 1$, the force has the form of a repulsive power-law. We have adopted the repulsive power-law for for L1 and L2 systems for which $\xi > 1$. While the value of a for the L1 case is taken to be 1.40, it is 1.50 for the L2 case. The power b has been taken to be 12 for both the cases. The structure factor for L1 obtained from simulation compares well with the experimental result at low q but fails to capture the behavior near the second peak (see Fig. 7(c)). The dimensionless PGNP density in the simulation is $\rho = 0.20$ and the temperature is $T = 1.0$. Fig. 7(d) exhibits the comparison of $S(q)$ for L2 case using the power-law form at dimensionless density $\rho = 0.09$. In the case of L2, the ratio of the number of polymers to the number of PGNPs is larger than that for L1, but Model-Y fails to describe the experimental data beyond the first peak of $S(q)$. The values of PGNP size $a\sigma$ used to bring the simulation result for q^* in agreement with the experimentally observed value are 37.3 nm and 35.2 nm in panels (c) and (d), respectively. The comparisons between experimental and numerical data shown in Fig. 7 indicate that (a) Model-X provides better agreement with experimental data than Model-Y for the L1 sample; and (b) the degree of agreement with experimental data decreases for both Model-X and Model-Y as the density of matrix polymers is increased in going from sample L1 to L2 and L3 (data not shown here). Implications of these observations are discussed in section IIID below.

C. Effective interaction between PGNPs

In this section, we describe the effective interactions between two PGNPs in the presence of matrix polymers of different densities. The effective interactions between two PGNPs has been obtained from

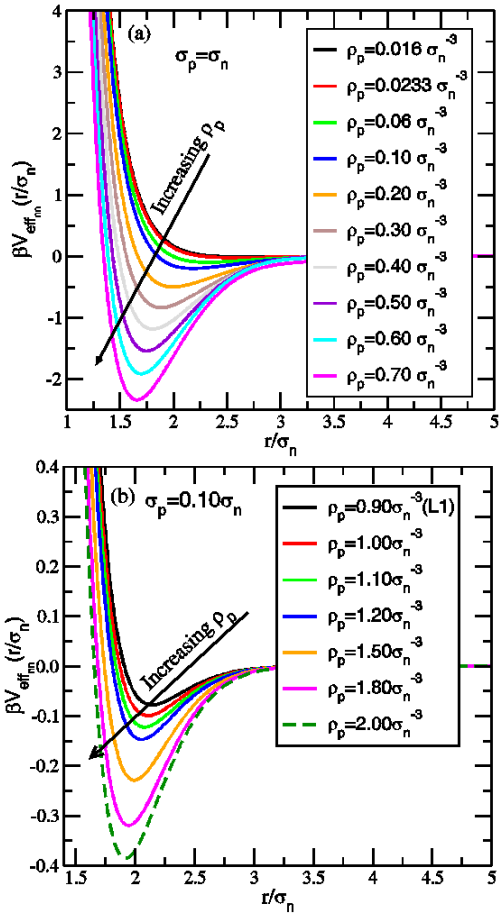

FIG. 8. The effective interactions between two PGNPs in the presence of different densities of matrix polymers for (a) $\sigma_p/\sigma_n = 1.00$ and (b) $\sigma_p/\sigma_n = 0.10$.

$$\beta V_{eff}(r) = -\ln\left[g_{nn}(r; f, \rho_n \to 0, \rho_p)\right] \tag{20}$$

where the radial distribution function $g_{nn}(r)$ has been obtained using integral equation theory described in section II D. For the calculation of $g_{nn}(r)$, we have used the potential of model- X. Fig. 8(a) shows the effective interaction between PGNPs in the presence of matrix polymers with size the same as that of the polymers grafted to the nanoparticles *i.e.* similar to H case. The matrix polymer density $0.016\sigma_n^{-3}$, $0.023\sigma_n^{-3}$ and $0.06\sigma_n^{-3}$ correspond to the situations of H1, H2 and H3, respectively. While H1 shows that the $V_{eff}(r)$ is weakly attractive, it starts developing an attractive well with the increase of matrix polymer density *i.e.* going from H1 to H2 and then to H3. If the matrix polymer density is further increased, the depth of the attractive well increases as well. In Fig.- 8(b) the effective interactions

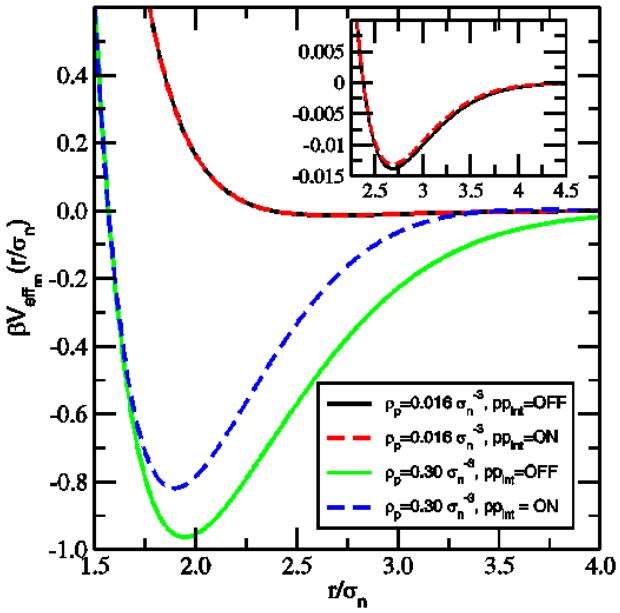

FIG. 9. Comparison of effective interactions between two PGNPs in the presence of matrix polymers with or without polymer-polymer interactions at densities $\rho_p = 0.016\sigma_n^{-3}$ and $\rho_p = 0.30\sigma_n^{-3}$. While at low density the effect of polymer-polymer interaction is negligible, at large polymer density the $V_{eff}(r)$ is more negative in the absence of polymer-polymer repulsive interactions. The size ratio $\sigma_p/\sigma_n = 1.00$. Inset: Enlarged plot for $\rho_p = 0.016\sigma_n^{-3}$. The pp_{int}=OFF and ON means the polymer-polymer interaction is absent and present respectively.

between PGNPs has been shown for the case where the size of the matrix polymer is $1/10^{th}$ of that of the grafted polymer (L based systems). The matrix polymer density $\rho_p = 0.90\sigma_n^{-3}$ corresponds to the L1 case. We observe that for this case we have an attractive well of depth of order $0.1k_BT$. In the case of L2 the matrix polymer density is much higher compared to the L1 case and therefore, it is very clear from the figure that the $V_{eff}(r)$ has an attractive well of large depth. We have also studied the effect of polymer-polymer interaction on the effective interactions between two PGNPs. Fig. 9 exhibits the $V_{eff}(r)$ between PGNPs with and without polymer interactions for matrix polymer density $\rho_p = 0.016\sigma_n^{-3}$ and $\rho_p = 0.30\sigma_n^{-3}$. In Fig 9, pp_{int}=OFF and ON represent the cases when the polymer-polymer interaction is absent and present respectively. The size of a polymer in the matrix is the same as that of a grafted polymer. From this figure it is clear that while the effect of polymer-polymer interactions on the $V_{eff}(r)$ is negligible at low matrix polymer density, it has considerable effect on the $V_{eff}(r)$ at large density. The depth of the effective interaction is larger in the

absence of the polymer-polymer interactions compared to the case when there is polymer-polymer interaction, of the form given in Model-X which is basically repulsive.

D. Microscopic origin of discrepancies

Our MD simulations are able to reproduce the structure of pure PGNP using Model-X and blends with $\xi = 0.14$ (H series samples) could also be modeled reasonably well using both Models-X and -Y. While simulations using both models provide reasonable agreement with experimental results for the L1 case, the agreement deteriorates significantly for L2 and L3. A possible reason why these models do not work for L2 is that the ratio of the number of matrix polymers to the number of PGNPs in the case of L2 is much larger compared to that for L1 and the H series samples. The failure of Model-X in describing the experimentally observed behavior in systems (such as L2) with a large density of matrix polymers may be a consequence of the simple approximation used in this model to describe linear polymers. In model-X, the matrix polymers are considered to be star polymers with $f = 2$, with a slight modification of the long-distance part of the interaction between two matrix polymers (Gaussian for $f = 2$, while Yukawa for large f). This approximation affects both the interaction between two matrix polymers and the interaction of matrix polymers with the PGNPs. A proper description of these interactions becomes more important as the density of matrix polymers is increased. We have seen that with the increase of the matrix polymer density, the effective interaction between two PGNPs in Model-X develops an attractive well and the depth of this well increases with the increase of chain density. The approximate potentials in Model-X may not be appropriate for describing this extreme situation. As shown in Fig. 9, the effective interaction between two PGNPs is sensitive to the interaction between polymers at high matrix polymer densities. Therefore, any error in the description of the interactions between two matrix polymers and between a PGNP and a matrix polymer would affect the structure more significantly if the density of matrix polymers is high, as in samples L2 and L3.

For Model-Y, the agreement between numerical and experimental results is reasonably good for samples in the H series. This is not surprising in view of the fact that for these samples, the interaction between PGNPs is of the Lennard-Jones type in Model-Y, which is similar to the effective interaction in Model-X, which provides a good description of the

experimental data. For sample L1, the repulsive power-law potential of Model-Y provides a reasonable fit to the experimental data for $S(q)$, but the fit is not as good as that obtained for Model-X. The fits become much worse for L2. The reason for the failure of Model-Y in these cases is not completely clear. It is possible that many-body interactions among the PGNPs, neglected in Model-Y because only two PGNPs in a melt of linear polymers were considered in the simulations leading to this model, play an important role when the density of matrix polymers is high (as in samples L2 and L3).The possible importance of such many-body interactions in this system was mentioned in Ref.[18].

When we compare the two models, one important contrast is that while for the H series systems with low density of matrix polymers, the effective potential between PGNPs is purely repulsive in Model-X, it is of the Lennard-Jones type with an attractive part in Model-Y. Both models, however, produce similar structure factors that compare reasonably well with experimental results. As the chain density is increased for samples in the H group, Model-X also shows an effective potential with an attractive part, similar to Model-Y. So, it appears that both models are giving the same form of the effective potential at large chain densities. This makes sense, as the force in Model-Y is obtained at very large matrix polymer density. For L systems, on the other hand, Model-X shows an effective potential with an attractive part, but Model-Y predicts a purely repulsive potential of inverse power law form. A potential with an attractive part, representing depletion effects, appears to be more physical for samples in the L series. This is perhaps the reason for the observation that the simulation data for the L1 system obtained from Model-X provide a better fit to the experimental data for $S(q)$ than the data obtained from Model-Y. More detailed comparison between the two models is not possible because Ref.[18] considers only cases of $\xi = 1$ and $\xi = \frac{1}{7}$ and a single (large) density of matrix polymers.

IV. SUMMARY AND OUTLOOK

In conclusion, we have studied the structure and effective interactions of suspensions of PGNPs and PGNP-polymer mixtures using the combination of SAXS, MD simulations and integral equation theory. The main conclusions of the present work are summarized below:

1. It is shown that Model-X captures the structure factor of PGNPs reasonably well, further confirming the structural similarity between PGNPs and star polymers as shown earlier[6].

Based on experimental and simulation data of H systems, it is clear that PGNPs in the presence of large size matrix polymers exhibit depletion interaction. As the density of PGNPs decreases going from H1 to H3, the effect of depletion interaction on the structure factor gets counterbalanced by the effect of lowering density. Similar situation should be present for L systems as well where $S(q)$ peak position remains unchanged going from L1 to L2. Hence, for both ξ=0.14 and 2.76, the PGNPs in the presence of matrix polymers exhibit depletion behaviour, unlike in PNCs where entropic contributions due to graft-matrix interactions dominate the behavior.

2. Both Model-X and Model-Y capture the experimental structure factor for blends with low density of added polymers (all the fraction with ξ=0.14 and L1). However, for blends with high density of added polymers, neither of the two models is able to reproduce the experimental structure factor, indicating a failure of the models. Model-X treats a matrix polymer as another star polymer with $f = 2$, with the long-distance part of the interaction changed from Yukawa to Gaussian. This may not be enough to mimic polymer-polymer and polymer-PGNP interactions, especially at large densities of matrix polymers. We have shown that polymer-polymer interaction affects the effective PGNP-PGNP interaction for large matrix density. Hence, it is important to model the linear polymers in a better way if the density of matrix polymers is high. This could be a reason why Model-X fails at large matrix polymer density but works for low matrix polymer density. For Model-Y, the effective forces might be different when more than two PGNPs are present, especially at large matrix polymer density, which may lead to many-body interactions among the PGNPs.

Our investigation suggests that a new model is required to study the diversity in the structure of PGNP and PGNP-polymer mixtures, especially at intermediate and high polymer densities.

V. ACKNOWLEDGEMENTS

Authors thank the Department of Science and Technology, India for the financial support and Saha Institute of Nuclear Physics, India for facilitating the experiments at the PETRA-III, Hamburg, Germany. The authors would also like to acknowledge Institute Nanoscience

Initiative (INI), IISc for providing access to TEM facilities and Central facility, Department of Physics for Thermogravimetric measurements.

REFERENCES

[1]S. K. Kumar, N. Jouault, B. Beniceweicz, & T. Neely, *Macromolecules*, **46**,3199, (2013)

[2]S. Chandran, N. Begam and J. K. Basu, *J. App. Phys.*, **116**(22), 222203, (2014)

[3]P. Akcora, H. Liu, S. K. Kumar, J. Moll, Y. Li, B. C. Benicewicz, L. S. Schadler, D. Acehan, A. Z. Panagiotopoulos, V. Pryamitsyn, V. Ganesan, J. Ilavsky, P. Thiyagarajan, R. H. Colby and J. F. Douglas, *Nature Materials*, **8**, 354 (2009)

[4]S. Srivastava, and J. K. Basu, *Phys. Rev. Lett.*, **98**, 165701 (2007)

[5]D. Vlassopoulos, E. Stiakakis and M. Kapnistos *Rheo. Rev.*, **49**, 179 (2007)

[6]S. Srivastava, S. Chandran, A. K. Kandar, C. K. Sarika, J. K. Basu, S. Narayanan, and A. Sandy, *J.Chem.Phys.*, **133**, 151105 (2010)

[7]S. Chandran, C. K. Sarika, A. K. Kandar, J. K. Basu, S. Narayanan, and A. Sandy, *J.Chem.Phys.*, **135**, 134901 (2011)

[8]S. Srivastava, A. K. Kandar, J. K. Basu1, M. K. Mukhopadhyay, L. B. Lurio, S. Narayanan, and S. K. Sinha , *Phy. Rev. E.*, **79**, 021408.(2009)

[9]A. K. Kandar, S. Srivastava, J. K. Basu, M. K. Mukhopadhyay, S. Seifert, and S. Narayanan, *J. Chem. Phys.*, **130**, 121102, (2009)

[10]A. K. Kandar, J. K. Basu, S. Narayanan and A. Sandy *Soft Matter*, **8**, 10055, (2012)

[11]T. Mandal, C. Dasgupta and P. K. Maiti, *J. Chem. Phy.*, **141**, 144901 (2014)

[12]C.M. Wijmans, F.A.M.Leermakers, and G.J.Fleer, *Langmuir*, **10**, 4514 (1994)

[13]F. LoVerso, S. A. Egorov, and K. Binder, *Macromolecules*, **45**, 8892 (2012)

[14]S. A. Egorov, and K. Binder, *J. Chem. Phy.*, **137**, 094901 (2012)

[15]C. Durand-Gasselin, R. Koerina, J. Riegerb, N. Lequeux and N. Sanson, *J. Coll. and Int. Sci.*, **434**, 188, (2014)

[16]C. Chevigny, F. Dalmas, E. D. Cola, D. Gigmes, D. Bertin, F. Bou, and J. Jestin, *Macromolecules*, **44**, 122 (2011)

[17]D. Dukes, Y. Li, S. Lewis,B. Benicewicz, L. Schadler, and S. K. Kumar, *Macromolecules*, **43**, 1564 (2010)

[18]D. Meng, S. K. Kumar, J. M. D. Lane and G. S. Grest, *Soft Matter*, **8**, 5002 (2012).

[19]A. Wilk, S. Huismann, E. Stiakakis, J. Kohlbrecher, D. Vlassopoulos, C.N. Likos, G. Meier, J.K.G. Dhont, G. Petekidis and R. Vavrin, *Eur. Phys. J. E*, **32**, 127 (2010)

[20]E. Stiakakis, D. Vlassopoulos, C .N . Likos, J. Roovers, G. Meier, *Phys.Rev. Lett.*, **89**, 208302 (2002)

[21]M. Camargo, S. A. Egorov and C. N. Likos, *Soft Matter*, **8**, 4177 (2012).

[22]A. Arceo, L. Meli and P. F. Green, *Nano Letters*, **8**, 2271 (2008)

[23]S. Chandran, N. Begam, V. Padhmanaban and J. K. Basu, *Nat. Commun*, **5**, 3697 (2014)

[24]C. Durand-Gasselin, N. Sanson and N. Lequeux, *Langmuir*, **27**(20), 12329, (2011)

[25]A. Mujtaba, M. Keller , S. Ilisch , and H.-J. Radusch , M. Beiner , T. Thurn-Albrecht and K. Saalwchter, *ACS Macro Lett.*, **3**(5), 481, (2014)

[26]V. M. Litvinov, R. A. Orza, M. Klueppel, M. van Duin, and P. C. M. M. Magusin, *Macromolecules*, **44**(12), 4887 (2011)

[27]S. Fischer, A. Salcher, A. Kornowski, H. Weller, and S. Foerster, *Angew.Chem.Int.Ed.*, **50**, 7811 (2011)

[28]V. V. Ginzburg, *Macromolecules*, **46**, 9798 (2013)

[29]V. Ganesan, C. J. Ellison and V. Pryamitsyn, *Soft Matter*, **6**, 4010 (2010)

[30]A. Jayaraman, *J. Poly. Sci.: Part B: Poly. Phy*, **51**, 524, (2013)

[31]M. K. Corbierre, N. S. Cameron, M. Sutton, S. G. J. Mochrie, L. B. Lurio, A. Ruhm, and R. B. Lennox, *J. Am. Chem. Soc.*, **123**, 10411, (2001)

[32]E. Stellamanns, D. Meissner, M. Lohmann and B. Struth *J. Phy: Conf. Series*, **425**, 202007, (2013).

[33]J. L. Alessandrini and M. A. Carignano, *Macromolecules*, **25**, 1157 (1992).

[34]G. Beaucage, *J. Appl. Crystallogr.*, **28**, 717, (1995).

[35]G. Beaucage, *J. Appl. Crystallogr.*, **29**, 134, (1996).

[36]D. Brown and J. Clarke, *Molecular Physics*, **51**, 1243 (1984).

[37]R. L. C. Vink, A. Jusufi, J. Dzubiella and C. N. Likos, *Phys. Rev. E*, **72**, 030401 (2007).

[38]C. Mayer and C. N. Likos,*Macromolecules*,**40**, 1196 (2007).

[39]L. S. Ornstein and F. Zernike, *Proc. Acad. Sci. Amsterdam*, **17**, 793 (1914).

[40]J. P. Hansen and I. R. McDonald, *Theory of Simple Liquids, Academic Press, London* (2006).

[41]F. J. Rogers and D. A. Young, *Phys. Rev. A*, **30**, 999 (1984).

[42]J. K. Percus and G. J. Yevick, *Phys. Rev.*, **110**, 1 (1958).

[43]D. A. McQuarrie, *Statistical Mechanics, Viva Books Private Limited* (2003).

[44]K. N. Pham,A. M. Puertas, J. Bergenholtz, S. U. Egelhaaf, A. Moussad, P. N. Pusey, A. B. Schofield, M. E. Cates, M. Fuchs and W. C. K. Poon, *Science*, **296**, 104 (2002)

[45]T .Eckert and E. Bartsch, *Phys. Rev. Lett.*, **89**, 125701, (2002)

[46]A. N. Semenov, *Macromolecules*, **41**, 2243, (2008)

[47]S. Asakura and F. Oosawa, *J. Polym. Sci. Polym. Symp.*, **33**, 183, (1958)

[48]T. B. Martin, P.M. Dodd and A. Jayaraman *Phys. Rev. Lett.*, **110**, 018301, (2013)